Cell Research (2008) 18:589-599.

www.nature.com/cr

ORIGINAL ARTICLE

The *Arabidopsis MutS* homolog *AtMSH5* is required for normal meiosis

Xiaoduo Lu[1, 2, *], Xiaolin Liu[2, 3, *], Lizhe An[1], Wei Zhang[4], Jian Sun[2, 3], Huijuan Pei[1], Hongyan Meng[2, 3], Yunliu Fan[2, 3], Chunyi Zhang[2, 3]

[1]School of Life Sciences, Lanzhou University, Lanzhou 730000, China; [2]Biotechnology Research Institute, Chinese Academy of Agricultural Sciences, Beijing 100081, China; [3]National Key Facility for Crop Gene Resources and Genetic Improvement (NFCRI), Beijing 100081, China; [4]School of Life Sciences, Shanghai University, Shanghai 200444, China

MSH5, a member of the *MutS* homolog DNA mismatch repair protein family, has been shown to be required for proper homologous chromosome recombination in diverse organisms such as mouse, budding yeast and *Caenorhabditis elegans*. In this paper, we show that a mutant *Arabidopsis* plant carrying the putative disrupted *AtMSH5* gene exhibits defects during meiotic division, producing a proportion of nonviable pollen grains and abnormal embryo sacs, and thereby leading to a decrease in fertility. *AtMSH5* expression is confined to meiotic floral buds, which is consistent with a possible role during meiosis. Cytological analysis of male meiosis revealed the presence of numerous univalents from diplotene to metaphase I, which were associated with a great reduction in chiasma frequencies. The average number of residual chiasmata in the mutant is reduced to 2.54 per meiocyte, which accounts for ~25% of the amount in the wild type. Here, quantitative cytogenetical analysis reveals that the residual chiasmata in *Atmsh5* mutants are randomly distributed among meiocytes, suggesting that *AtMSH5* has an essential role during interference-sensitive chiasma formation. Taken together, the evidence indicates that AtMSH5 promotes homologous recombination through facilitating chiasma formation during prophase I in *Arabidopsis*.

***Keywords*:** meiosis, recombination, chiasmata, *AtMSH5*, *Arabidopsis*

Cell Research (2008) **18**:589-599. doi: 10.1038/cr.2008.44; published online 1 April 2008

Introduction

Eukaryotic cells such as those from yeast, *Caenorhabditis elegans*, mice, humans and *Arabidopsis* possess DNA mismatch repair (MMR) proteins. These MMR proteins are crucial to the fidelity of both DNA replication and the chromosome interactions that involve a series of interrelated events, including chromosome paring, synapsis and recombination. They are classified as MutS and MutL homologs, which refer to the *Escherichia coli* MutS and MutL post-replicative MMR model systems [1]. MutS proteins are heterodimers that recognize and bind mismatched base pairs that arise from erroneous DNA replication or from recombination, whereas MutL may act as a bridging factor that binds to the DNA-MutS complex and is required for triggering excision and re-synthesis of the error-containing DNA strand [2].

In the budding yeast *Saccharomyces cerivisiae*, there are six MutS homologs. Five of these genes (*Msh2-6*) encode proteins that act on nuclear DNA, whereas *Msh1* is required for the stability of the mitochondrial genome [3, 4]. Unlike other MutS family members, Msh4 and Msh5 do not need to recognize mismatched base pairs; instead, it has been proposed that the ability to recognize aberrant DNA structures is modulated in these proteins through evolution. They can recognize recombination intermediates such as Holliday junctions, which are four-stranded DNA structures, and reduce the free energy of these intermediates to facilitate recombination [5, 6]. Mutants of *Msh4* and/or *Msh5* display reduced levels of meiotic crossover and spore viability by as much as 30-50% of the wild type.

Homologs of *Msh4* and/or *Msh5* have also been found

*These two authors contributed equally to this work.
Correspondence: Chunyi Zhang
Tel: +86-10-62135337; Fax: +86-10-62136981
E-mail: chunyi.zhang@caas.net.cn
Received 4 September 2007; revised 24 October 2007; accepted 16 November 2007; published online 1 April 2008

in nematodes [7], mice [8, 9], humans [10, 11] and *Arabidopsis* [12]. It has been reported that MSH4 and MSH5 function in mammals in a similar way to yeast; they function as heterodimers to specifically promote crossing-over during meiotic recombination. Mouse MSH5 is required for chromosome pairing and synapsis in male and female meiosis [8, 9] and can physically interact with MSH4 to form heterodimers [13]. Mice that carry disrupted *Msh5* have been reported to display defective chromosome synapsis, resulting in testicular and ovarian degeneration and, therefore, male and female sterility [8]. In humans, genetic variations in *MSH5* are associated with IgA deficiency and common variable immune deficiency, which are probably due to the regulation of Ig class switch recombination [14].

Previously, a homology-based search revealed seven *MutS* homologs, which were designated *AtMSH1-7*, and at least four MutL homologs, *AtMLH1*, *AtMLH3*, *AtMLHX* and *AtPMS1*, in *Arabidopsis*. *AtMSH1* is involved in maintenance of the mitochondrial genome [15]. AtMSH2 has an anti-recombination effect, which is a function of homolog sequence divergence [16], and is essential for maintaining nuclear genome integrity during diploid growth by limiting the accumulation of insertion/deletion mutations during seed-to-seed propagation [17]. *Arabidopsis* plants deficient in *AtMSH4* exhibited normal vegetative growth but severe reduction in fertility, which is consistent with delayed and incomplete chromosome prophase I synapsis. Moreover, metaphase I chiasma frequency was greatly reduced to as much as ~15% of the wild type, leading to univalence and nondisjunction. However, although it is known that AtMSH2-AtMSH3, AtMSH2-AtMSH6 and AtMSH2-AtMSH7 form heterodimers and bind to various forms of DNA base pair mismatches [18], the biological function of other *Arabidopsis MutS* homologs, including *AtMSH3*, *AtMSH5*, *AtMSH6* and *AtMSH7*, awaits further investigation.

In this study, we demonstrate that an *Arabidopsis* T-DNA insertion mutant *Atmsh5* exhibits defects in male meiosis, which include the presence of numerous univalents, a random distribution of residual chiasmata and decreased levels of chiasma frequency during prophase I of meiotic division.

Results

Isolation and characterization of a T-DNA insertion Atmsh5 mutant

In our previous study of the gene expression pattern of *AtNPC2* (unpublished observations), the promoter fused

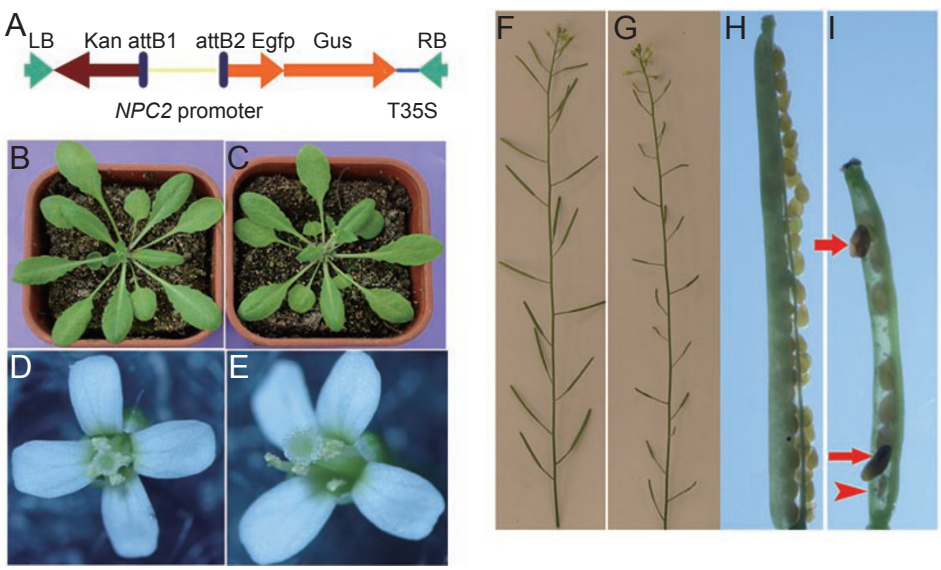

Figure 1 Phenotypic characterization of the T-DNA insertion mutant. **(A)** Schematic representation of the *NPC2* promoter *GFP-GUS* fusion construct. The scheme illustrates the construct structure only, and is not to scale. LB and RB represent the left border and right border on T-DNA. attB1 and attB2 represent the two short stretches of sequences that participate in the recombination reaction of the Gateway system. T35S indicates 35S terminator. **(B)** Wild-type plant. **(C)** T-DNA insertion mutant plant, with vegetative growth that is similar to that of the wild type. **(D)** Wild-type flower. **(E)** T-DNA insertion mutant flower in which all flower organs appear normal. **(F)** Siliques of the wild-type plant. **(G)** Siliques of the T-DNA insertion mutant are smaller than those of the wild type. **(H)** A dissected silique of the wild type, showing normal developing seeds. **(I)** A dissected silique of the T-DNA insertion mutant, showing only a few developing seeds.

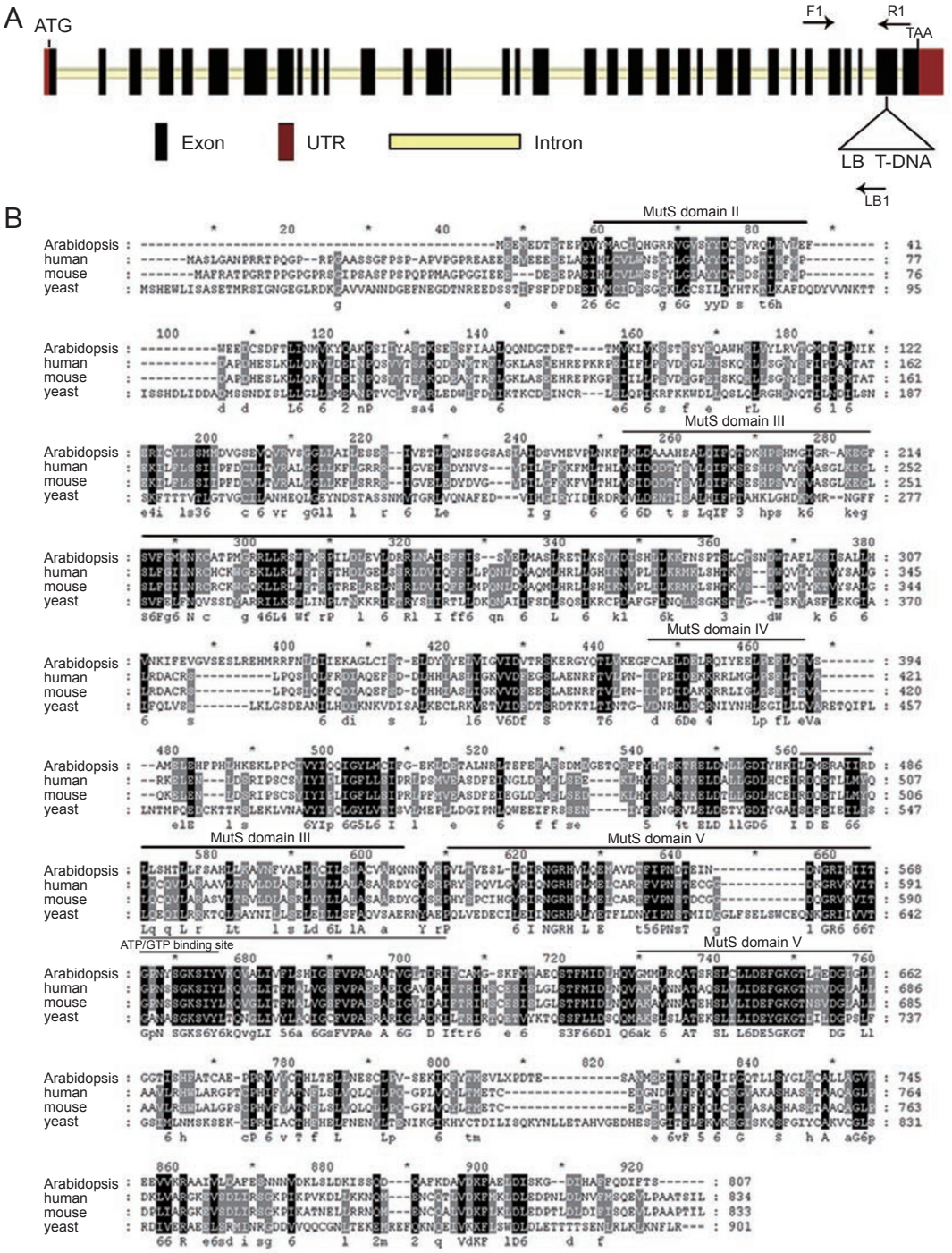

Figure 2 *AtMSH5* gene structure and its homologs from humans, mice and *C. elegans*. **(A)** Exon/intron structure of the *AtMSH5* gene. Solid black boxes represent exons. 5′ UTR and 3′ UTR are shown in solid red boxes. The triangle indicates the site of T-DNA insertion, and the two arrows show the positions of the primers that were used for RT-PCR analysis of *AtMSH5* expression (Figure 3). **(B)** Alignments of the deduced amino-acid sequences of AtMSH5 with its homologs in humans, mice and yeast. These four MSH5 homologs were aligned using the ClustalW program from the European Bioinformatics Institute (http://www.ebi.ac.uk/clustalw/). 3-level conservation shading was accomplished using the GeneDoc program. Residues that are conserved across all four sequences are shaded black; residues that are conserved across two or three sequences are shaded light gray or dark gray, respectively. Consensus sequences are shown underneath; conserved amino-acid groups are as follows: 1 = DN, 2 = EQ, 3 = ST (hydroxylated), 4 = KR (basic), 5 = FYW (aromatic) and 6 = LIVM (aliphatic or M).

with the *GFP-GUS* gene was transformed into *Arabidopsis* (Columbia) via *Agrobacterium*-mediated transformation (Figure 1A), and tens of independent transgenic plants were obtained. One of these transgenics resembled the wild type during vegetative development under normal growth conditions, and its flowers had normal morphology, including normal floral organ identity and number (Figure 1B-1E). However, drastically reduced silique length and seed-set, compared with the wild type, was observed in this transgenic (Figure 1F-1I), which is indicative of probable fertility defects. Mean silique length was reduced to 7.5 ± 0.59 mm in the transgenic (n = 150 from 10 individual plants), compared with 12.0 ± 0.54 mm in the wild type, and the mean seed-set was only 9 ± 1.34 per silique, accounting for 16.6% of the normal seed-set in the wild-type Columbia ecotype (n = 150 from 10 individual plants). Some of the mutant seeds were abnormal in appearance with dark (red arrow) and shrunken (red arrowhead) seed coats (Figure 1I).

To identify the gene that is mutated in the transgenic, we sought to identify the position of the T-DNA insertion through PCR-walking (see Materials and Methods). Two PCR products were obtained using *Sca*I- and *Eco*RV-digested genomic DNA as templates. Sequencing of the two PCR products confirmed the T-DNA insertion and precisely mapped both of the products to a position 87 523 bp along the BAC clone MQC1 (locus At3g20475). Results from an NCBI blast search indicate that this locus encodes a putative *Arabidopsis thaliana* MutS-like protein 5 (AtMSH5), and that the T-DNA has inserted into exon 33 (Figure 2A). The T-DNA insertion was confirmed through amplification of the flanking region using the primer specific to the left border of the T-DNA and the primer specific to the genomic DNA sequences that were isolated through PCR-based walking. PCR amplification from genomic DNA of the homozygous mutant line confirmed the absence of the wild-type allele (data not shown). RT-PCR analysis using the gene-specific primers did not detect *AtMSH5* transcripts even after 33 cycles of amplification in the T-DNA insertion mutant (Figure 3).

Figure 3 *AtMSH5* expression is tissue specific. RT-PCR analysis of *AtMSH5* transcript expression in the wild-type leaf (L), stem (S), open flower (F) and meiotic floral bud (B), and in the *Atmsh5* mutant meiotic floral bud (mut). The tubulin gene was used as a control.

To confirm the causal relationship between disruption of the *AtMSH5* gene and reduced fertility, the *Atmsh5* mutant was crossed with the wild-type male or female parent, and co-segregation of the phenotype with the genotype was analyzed in the F2 progeny. As many as 92 F2 progeny were genotyped using both the T-DNA left border specific primer and the primers designed against the *AtMSH5* genomic DNA sequence to detect the homozygosity of the mutated *AtMSH5* gene; they were then phenotypically scored for their fertility. The results show that the mutation was monogenic and recessive, and that the T-DNA insertion in the *AtMSH5* gene was tightly linked with the mutant phenotype ($P < 0.001$) (data not shown).

The gene structure of Arabidopsis MSH5

To identify the gene structure of the putative *MSH5* in *Arabidopsis*, 5′- and 3′-RACE PCR analyses were performed to isolate full-length cDNA using primers specific to parts of the coding region sequences, and the results confirmed the cDNA sequences with open reading frames of 2 424 bp, released by Genbank (accession number EF471448).

Aligning the cDNA sequence against the published genomic DNA sequence of At3g20475 (TAIR) allowed the determination of the intron/exon gene structure. *AtMSH5* comprises 34 exons and 33 introns (Figure 2A), of which there are 14 exons smaller than 50 bp. This is different from the predicted gene structure, which contains only 14 exons that are 990 bp long and 13 introns (NM112939). The predicted gene omits the experimentally derived exons 1-20, and the predicted 5′ UTR falls into exon 20.

AtMSH5 comprises conserved MutS domains

The *AtMSH5* open reading frame encodes a predicted protein that consists of 807 amino-acid residues with a molecular mass of 91.09 kDa and a theoretical pI of 5.08. Comparison of this amino-acid sequence with other MutS homologs that are deposited in the Genbank databases indicated that it is most related to human MSH5, with 31% identity and 50% similarity (Figure 2B). It also has significant homology with MSH5 in mouse (30% identity and 50% similarity) and in yeast (29% identity and 47% similarity). A motif scan (http://myhits.isb-sib.ch/cgi-bin/motif_scan) indicated that there is one ATP/GTP binding site (residues 569-576, also named the p-loop), and some highly conserved domains, including one MutS family signature (residues 642-658), one MutS domain II (residues 13-41), two MutS domain III (residues 180-283 and 476-520), one MutS domain IV (residues 371-392) and three MutS domain V (residues 523-610, 635-661 and 562-576). These domains are

present in meiosis-specific MutS homologs from yeast, humans and *C. elegans*. However, AtMSH5 is devoid of MutS domain I, which is critical for MMR activity. AtMSH5 also contains an ATPase domain, encompassed in domain V, with an ATP/GTP binding site (GPNYSGKS).

AtMSH5 expression is tissue-specific

Expression of the *AtMSH5* transcript was examined in different tissues using RT-PCR with gene-specific primers. Transcript expression was detected only in young floral buds at the meiotic stage, not in open flowers or vegetative tissues such as stems and leaves (Figure 3). This indicates that *AtMSH5* may play an important role in meiosis during a very narrow developmental window. These results are in accordance with those from other species such as yeast, where the expression of *MSH5* is detectable only during meiosis [5], and mouse, where the expression of *MuMSH5* is limited to the testes and ovaries [8].

Male and female fertility is affected in Atmsh5 mutants

In order to examine the effects of *Atmsh5* mutation on male and female fertility, five *Atmsh5* homozygous mutant plants were used as either the female or the male parent crossed with five wild-type plants. When the mutant was the female parent, there were 8 seeds per silique on average (n = 20), among which 30% were found to be abnormal in appearance. When the mutant was the male parent, 12 seeds per silique were observed on average (n = 15), among which 33% were abnormal (dark and shrunk). These crosses indicate that both male and female fertility is impaired in the *Atmsh5* mutant.

The viability of the *Atmsh5* pollen grains was checked using Alexander's staining solution. Almost half of the pollen grains were not viable (376 out of 707 mutant pollen grains: 53.2%), as indicated by blue staining (Figure 4). Embryo sac development was also perturbed in the *Atmsh5* mutant. In wild-type ovules, a single nuclear cell differentiates into the megaspore mother cell (MMC) (Figure 5A) and undergoes meiosis to produce four haploid megaspores, only one of which survives. This functional megaspore undergoes three mitotic divisions to produce an eight-nuclei coenocytic embryo sac, which will then cellularize into a seven-celled embryo sac (Figure 5C). Wild-type and *Atmsh5* mutant pistils were investigated using confocal laser scanning microscopy (CLSM). At the MMC stage, there was no difference between the wild type and the mutant (Figure 5A and 5B). At the mature female gametophyte stage, however, only 15% (n = 500) of the mutant ovules displayed normal female gametophytes. Embryo sacs containing one functional megaspore or one cell were observed in the remaining abnormal ovules in the mutant (Figure 5D and 5E).

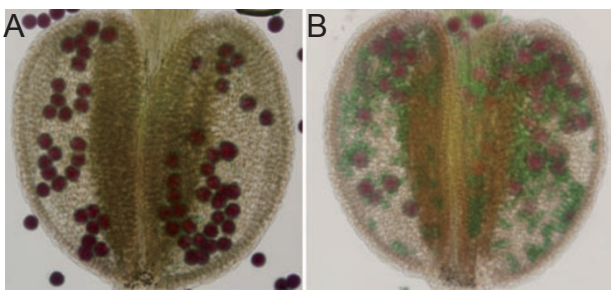

Figure 4 Pollen viabilities of the wild type and the *Atmsh5* mutant. Anthers of the wild type **(A)** and the *Atmsh5* mutant **(B)**, which are stained with Alexander's solution. The red-purple-stained cytoplasm indicates viable pollen grains, whereas the pollen cell wall is counterstained in green and the dead pollen grains are stained blue.

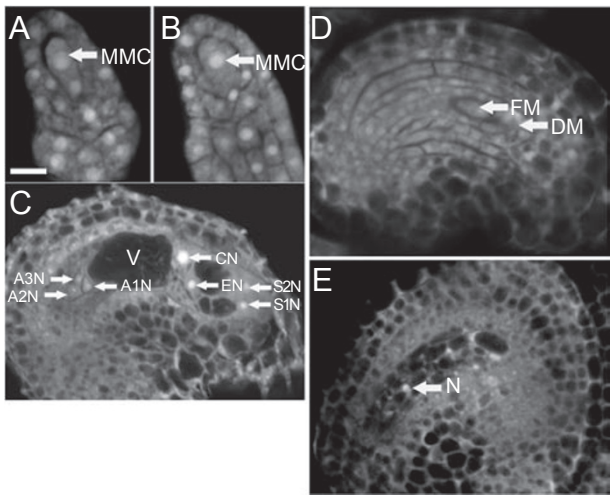

Figure 5 Ovule development revealed by confocal laser scanning microscopy (CLSM) in wild-type and *Atmsh5* mutant plants. **(A)** A wild-type female gametophyte at stage FG0. **(B)** An *Atmsh5* female gametophyte at FG0. **(C)** A mature ovule from a wild-type plant. **(D)** A one-functional megaspore embryo sac from an *Atmsh5* mutant plant. **(E)** An ovule without embryo sac from a *Atmsh5* mutant plant. MMC, megaspore mother cell; AN, antipodal nucleus; CN, central cell nucleus; EN, egg nucleus; SN, synergid nucleus; V, vacuole; FM, functional megaspore; DM, degenerating megaspore.

Disruption of AtMSH5 causes abnormal male meiosis

As the mutant had shorter siliques and less seed-set than the wild type, it is speculated that *AtMSH5* may be necessary for normal meiosis. Male meiosis in wild-type and mutant plants was compared using chromosome

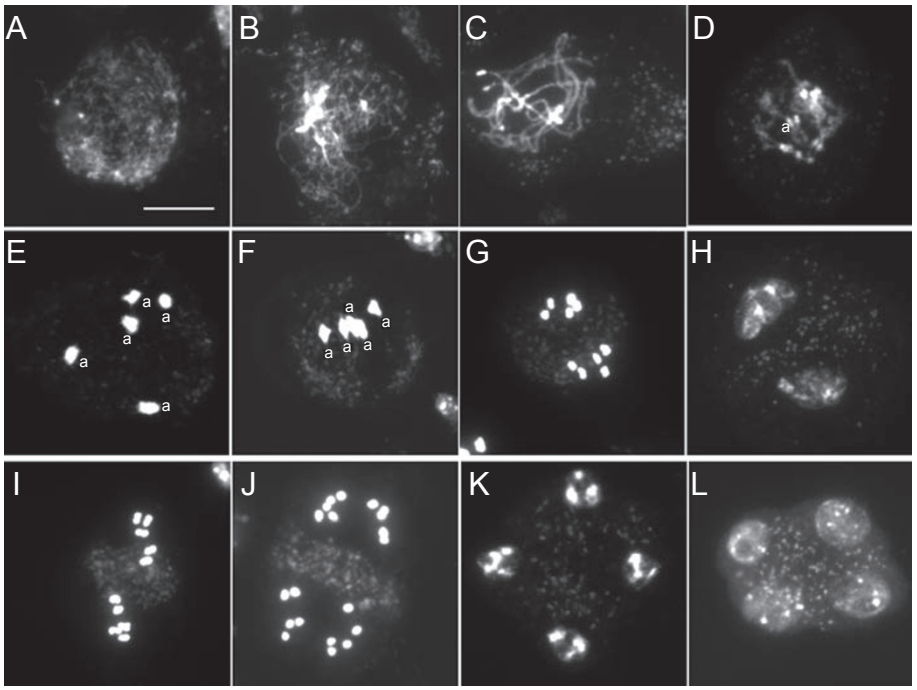

Figure 6 Male meiosis in wild-type *Arabidopsis* plants. **(A)** Leptotene stage. **(B)** Zygotene stage. **(C)** Pachytene stage. **(D)** Late diplotene stage. **(E)** Diakinesis stage. **(F)** Metaphase I stage. **(G)** Anaphase I stage. **(H)** Telophase I stage. **(I)** Metaphase II stage. **(J)** Anaphase II stage. **(K)** Telophase II stage. **(L)** Tetrad stage. "a" indicates double crossover bivalents. Bar = 10 μm.

spreads stained with 4′,6-diamidino-2-phenylindole (DAPI). In wild-type plants, male meiosis I started with the condensation of chromatin, forming distinct thin chromosome threads at the leptotene stage (Figure 6A) and undergoing synapsis at the zygotene stage (Figure 6B). Juxtaposed homologs were observed at the pachytene stage (Figure 6C). Chromosomes then underwent further condensation at the diplotene and diakinesis stages (Figure 6D and 6E) and aligned at the division plane at metaphase I (Figure 6F). At anaphase I, homologous chromosomes segregated and moved to opposite poles (Figure 6G), and eventually tetrads formed at anaphase II (Figure 6H-6L). In mutant plants, the early development stages of meiotic nuclei, in other words from leptotene to pachytene, appeared to proceed normally (Figure 7A-7C). The presence of unpaired homologous chromosomes was observed at the diplotene stage in the mutant (Figure 7D), and numerous univalents were observed at diakinesis/metaphase I (Figure 7E and 7F), which is in contrast to the five bivalents that were observed during the corresponding meiotic stages in the wild-type meiocytes (Figure 6E and 6F). At metaphase I in the mutants, the bivalents aligned at the equator of the spindle, whereas the univalents were distributed randomly (Figure 7F), behaving differently from the wild type (Figure 6F). During anaphase I, the univalents segregated abnormally, resulting in an uneven distribution of univalents (Figure 7G and 7H). At anaphase II, segregation of the sister chromotids was also disturbed (Figure 7J and 7K), characterized strikingly by the presence of abnormal numbers of chromosomes in polyads (Figure 7L). It was found that there were often three to six nuclei formed in the mutant meiotic cells in contrast to four in the wild type. Taken together, the characteristics of the resulting mutant nuclei with abnormal chromosome numbers may account for the reduction in pollen viability and fertility described previously.

The Atmsh5 mutant exhibits reduced numbers of chiasmata and bivalents

At prophase I, the mutant meiocytes exhibited a reduction in chiasma frequency compared with the wild-type meiocytes. The structure of the bivalents was used to count the chiasmata as described by Sanchez-Moran *et al*. [19]. The distribution of the number of chiasmata per cell in the *Atmsh5* mutant and in the wild type is shown graphically in Figure 8. Counts from 50 *Atmsh5* mutant pollen mother cells from 5 inflorescences showed an average of 2.54 chiasmata per cell (0.51 per chromosome pair), compared with an average of 9.85 chiasmata per cell in wild-type meiocytes (1.97 per chromosome pair) (Figure 8A and 8B). In fact, 12% of *Atmsh5* mutant cells lacked chiasmata completely. As expected, this resulted in frequent errors in chromosome segregation and nuclei with variable chromosome numbers from both the first and second division (Figure 7). Despite the low mean chiasma frequency in the *Atmsh5* mutant, the number of chiasmata per cell was variable, ranging from 0 to 8. The

number of chiasmata per wild-type meiocytes (n = 67) was close to the average, and never less than 8 nor more than 12 chiasmata per cell (Figure 8A). As numerous univalents were present in the *Atmsh5* mutant meiocytes at late prophase I to metaphase I (Figure 7E and 7F), we next counted the number of bivalents on a single-celled basis. Among 50 *Atmsh5* meiocytes at the diakinesis stage, 12% had no bivalents; 32%, 26%, 24%, 6% and 0% of the meiocytes were found to have 1, 2, 3, 4 and 5 bivalents, respectively, with an average of 1.8 bivalents per cell, compared with an average of 4.95 bivalents per cell in the wild type (Figure 8C).

Finally and more importantly, the chiasma distribution in the *Atmsh5* mutant was found to be close to the predicted Poisson distribution ($\chi^2_{(6)} = 9.08$, $P > 0.1$) (Figure 8B), suggesting a near random distribution of these residual chiasmata among cells. However, in the wild type, chiasma distribution deviated significantly from the predicted Poisson distribution ($\chi^2_{(11)} = 117.53$, $P < 0.001$) (Figure 8A).

Discussion

Unlike the *MSH1* and *MSH2* families of *MutS* homologs, in various organisms, including yeast, mice, *C. elegans* and humans, *MSH5* has been reported to be essential for the interrelated and consecutive events that occur during meiosis, such as chromosome pairing, synapsis and recombination, rather than to be involved in DNA MMR in somatic cells. To our knowledge, the function of the *MutS* homolog *MSH5* in plants has not yet been characterized. In this report, we describe the phenotype of an *Arabidopsis* mutant, *Atmsh5*. The mutant exhibits a drastic reduction in fertility, embodied by a smaller seed set and fewer viable pollen grains in the anthers than found in the wild type. Cytological observations of pollen mother cells over a range of meiotic stages revealed that abnormal meiosis occurs in the *Atmsh5* mutant. In addition, quantitative cytogenetical analysis of chiasma frequency and distribution shows that the residual chiasmata in *Atmsh5*, about 25% of the number in the wild type, are randomly distributed among the meiocytes.

AtMSH5 contains several conserved MutS domains. MutS domain I is the mismatch recognition site, and its absence eliminates recognition of mismatched DNA bases, as evidenced by the crystal structures of MutS-DNA complexes [20-22]. This domain is present in all MutS homologs and has an important role in MMR [23]. The absence of MutS domain I from *AtMSH5* leads us to propose that *AtMSH5* may not be involved in MMR. MutS domain II is a conserved intervening region that has been proposed to have a structural role, linking MutS domain I to DNA-association domain [20-22], and resembling RNase H and RNase H-like domains [24]. MutS domain III is entirely α-helical and central to the MutS structure, and is directly connected to domains II, IV and V by peptide bonds; it shares its most extensive interdomain contacts with domain V [22]. MutS domain IV is involved in

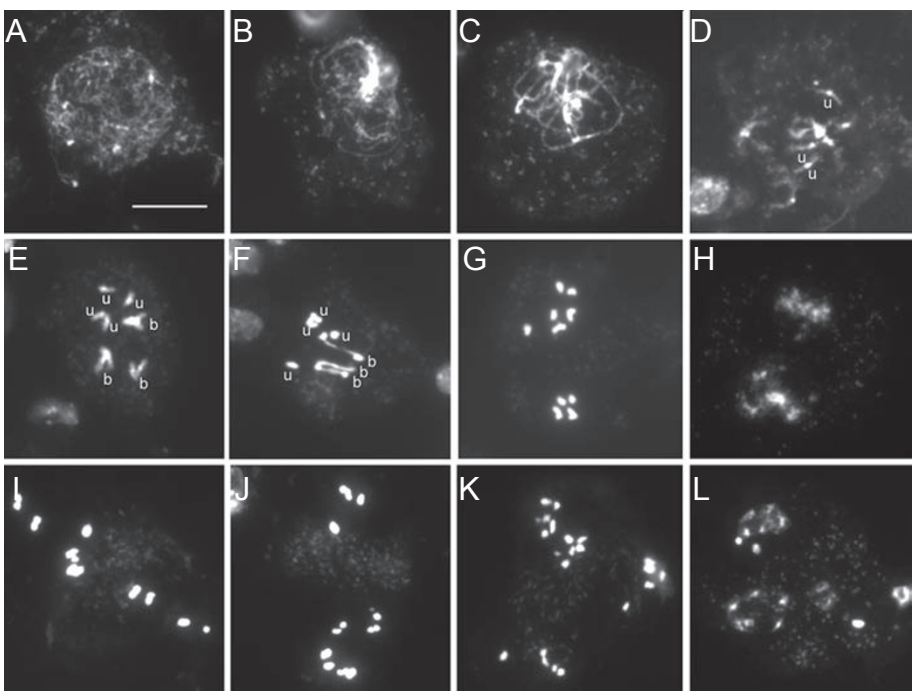

Figure 7 Male meiosis is disrupted in *Atmsh5* mutant plants. **(A)** Leptotene stage. **(B)** Zygotene stage. **(C)** Pachytene stage. **(D)** Late diplotene stage. **(E)** Diakinesis stage. **(F)** Late metaphase I stage. **(G)** Anaphase I stage. **(H)** Telophase I stage. **(I)** Metaphase II stage. **(J)** Anaphase II stage. **(K)** Telophase II stage. **(L)** Polyads stage. "b" indicates single crossover bivalents and "u" indicates univalents. Bar = 10 μm.

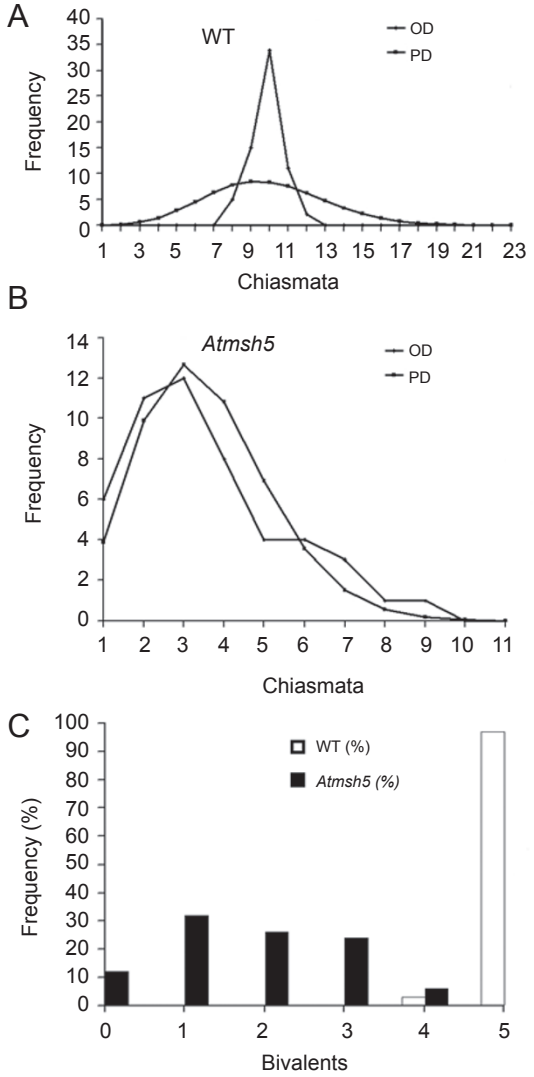

Figure 8 Distribution of chiasmata and bivalents in wild-type and *Atmsh5* mutant meiocytes. The frequency of chiasmata per meiocyte in the wild type **(A)** and in the *Atmsh5* mutant **(B)** is shown. OD, observed distribution. PD, predicted Poisson distribution. The frequency of bivalents per meiocyte in the wild type (white bars) and in the *Atmsh5* mutant (black bars) is presented in **(C)**.

DNA binding by clamping DNA crossovers or Holliday junctions, and is independently folded and appended to the core of MutS by flexible peptide linkages and limited interactions, which indicates a possibility for domain rearrangement [22, 25]. Domain V contains the helix-turn-helix motif that is involved in dimerization and ATPase activity [22, 26].

Loss of *Msh5* function in yeast leads to a specific deficit in crossover recombination events, but cells progress through meiosis and sporulate efficiently [5]. Likewise, progression through the meiotic prophase remains largely unperturbed in the *C. elegans msh5* mutant, leading to completion of meiosis and consequent survival of germ cells, apart from a severe reduction in crossover frequencies and a lack of chiasmata between homologous chromosomes [7]. By contrast, germ lines in the mouse *msh5* mutant exhibit an arrest of meiosis at the zygotene stage, which is characterized by impaired and aberrant chromosome synapsis, and is followed by apoptotic cell death [8]. These observations may indicate that there has been a functional divergence of MSH5 in various organisms.

S. cerevisiae msh4 and *msh5* mutant strains show a meiotic defect that is characterized by reduced spore viability, as well as increased levels of metaphase I nondisjunction and decreased levels of reciprocal exchange between homologous chromosomes [5, 27, 28]. Assessing spore viability and recombination in a yeast *msh4 msh5* double mutant led to a hypothesis that, rather than working in separate pathways, *Msh4* and *Msh5* function in the same process [5]. Therefore, Msh4 and Msh5 probably function as a heterodimeric protein complex in yeast meiotic cells [29].

Higgins *et al*. reported that the *Arabidopsis msh4* mutant exhibits a severe reduction in fertility, which is consistent with a meiotic defect. This defect is characterized by greatly reduced chiasma frequency, leading to univalence and nondisjunction, and by delayed and incomplete prophase I chromosome synapsis [12]. A similar phenotype has been described in *Arabidopsis mlh3* [30]. However, a detailed comparison of chiasma frequencies between *Atmsh4* and *Atmlh3* suggests that these two classes of MMR proteins have differing roles in crossover formation, even though it has been proposed that MutL homologs combine with the MutS homologs MSH4 and MSH5 in some structural role to promote meiotic crossovers.

It has been proposed that there are two distinct classes of crossovers in *S. cerevisiae* [27, 31], and that these two classes are promoted by biochemically distinct pathways [32]. Class I crossovers are interference sensitive and promoted by an *Msh4/5*-based complex, whereas class II crossovers are randomly distributed and promoted by an *MMS4/MUS81*-based complex. The decrease in crossover in yeast *mms4* and *mus81* mutants is modest, indicating that the majority of crossovers in wild-type yeast belong to class I [12, 32]. Several studies have suggested the existence of two pathways in *Arabidopsis*. Copenhaver *et al*. showed that genetically determined crossover distribution better fitted the hypothesis of two pathways [33]. Thereafter, two genes, *AtMSH4* and *AtMER3*/*AtRCK*, were identified as the components in class I crossovers [12, 34, 35]. Recently, *AtMUS81* was also

reported to be involved in interference-insensitive crossovers [36]. Our analysis of *Atmsh5* meiocytes indicates that although the number of chiasmata is greatly reduced, there is still a subset of chiasmata remaining that are independent of AtMSH5. The residual chiasmata are close to the Poisson distribution of random events, suggesting that AtMSH5 functions in the interference-sensitive pathway of meiotic recombination. The main phenotype of our mutant is similar to the *Atmsh4* mutant. Therefore, evidence from our phenotype strongly supports the idea that MSH4 and MSH5 are in the same pathway and probably form a heterodimer to facilitate chiasma formation.

Material and Methods

Plant materials

The *A. thaliana* ecotype Columbia was used in this study for wild-type analysis. Plants were grown in a greenhouse under supplementary light (cycles of 16 h of light and 8 h of darkness) at 22 °C.

Isolation of T-DNA flanking sequence tag

The T-DNA flanking sequence was amplified as described previously [37]. Two oligomers, ADPR1 and ADPR2, were mixed and incubated at 95 °C for 5 min and then at 28 °C for 5 min to allow them to anneal to form an adaptor. This adaptor was stored at –20 °C until it was used. The genomic DNA isolated from the *Arabidopsis* mutant was cut with blunt-end restriction enzymes, *Sca* I, *Hpa* I or *Dra* I, and ligated to the adaptor in the same reaction at a volume of 10 μL, with 100 ng DNA, 1 U digestion enzyme, 0.5 U T4 ligase, 1×T4 ligase buffer and 375 nM adaptor. PCR analysis was performed using the LB1 primer together with the AP1 primer, and then nested PCR was performed using the LB2 primer together with the AP2 primer. The PCR products were directly sequenced using the LB2 primer. The oligomers used to make the adaptor are listed as follows – ADPR1: 5′-GTA ATA CGA CTC ACT ATA GGG CAC GCG TGG TCG ACG GCC CGG GCT GGT-3′; and ADPR2: 3′-H_2N-CCC GAC CA-PO_4-5′. The primers used are listed as follows – AP1: 5′-GTA ATA CGA CTC ACT ATA GGG C-3′; AP2: 5′-ACT ATA GGG CAC GCG TGG T-3′; LB1: 5′-GAC TCT AGC TAG AGT CAA GCA GAT CGT-3′; and LB2: 5′-GAT CGA CCG GCA TGC AAG-3′.

Cloning the full-length AtMSH5 cDNA

Full-length *AtMSH5* cDNA was cloned according to the GeneRcer™ Kit (Invitrogen). In brief, 5 μg of the total bud RNA of the wild type was treated with calf intestinal phosphatase (CIP) to remove the 5′ phosphates, then the dephosphorylated RNA was treated with tobacco acid pyrophosphatase (TAP) to remove the 5′ cap structure from intact full-length mRNA. The GeneRacer™ RNA oligomers (5′-CGA CUG GAG CAC GAG GAC ACU GAC AUG GAC UGA AGG AGU AGA AA-3′) were then ligated to the 5′ end of the mRNA using T4 RNA ligase. Reverse transcription was carried out with the RNA oligomer-added mRNA, using AMVRT and the GeneRacer™ oligo-dT primer (5′-GCT GTC AAC GAT ACG CTA CGT AAC GGC ATG ACA GTG $(T)_{18}$-3′), to create RACE-ready first-strand cDNA with known priming sites at the 5′ and 3′ ends. To obtain the 3′ ends, the PCR reaction was performed using the first strand of cDNA as a template with a forward gene-specific primer (GSP1: 5′-AGT GTT AGA TCG CCG TCT CAA TGC TA-3′) and the GeneRacer™ 3′ primer (5′-GCT GTC AAC GAT ACG CTA CGT AAC G-3′), and then nested PCR was carried out with a forward gene-specific nested primer (GSP2: 5′-GTC TAT GAA CTG GTC ATT GGA GTC A-3′) and the GeneRacer™ 3′ nested primer (5′-CGC TAC GTA ACG GCA TGA CAG TG-3′). To obtain the 5′ ends, the PCR reaction was performed using a reverse gene-specific primer (GSP3: 5′-CTG TCA GGA CAG GCC TTA CGT AGT T-3′) and the GeneRacer™ 5′ primer (5′-CGA CTG GAG CAC GAG GAC ACT GA-3′), followed by nested PCR with a reverse gene-specific nested primer (GSP4: 5′-GCC TTC AGC AGG TGA GCC GAG AAC A-3′) and the GeneRacer™ 5′ nested primer (5′-GGA CAC TGA CAT GGA CTG AAG GAG TA-3′).

Semi-quantitative RT-PCR for transcript expression

A First Strand DNA Synthesis Kit (TOYOBO) was used to synthesize cDNA from DNase I-treated total RNA that was extracted from *Arabidopsis* wild-type (Col) leaf, stem, bud, flower, and bud tissue from *Atmsh5* mutant plants. Primers were designed to amplify a housekeeping gene *TUBLIN 4* to equalize RNA loading into the RT-PCR reaction. These were TUB4F: 5′-CGA AAA CGC TGA CGA GTG TA-3′ and TUB4R: 5′-CCT TGG GAA TGG GAT AAG GT-3′. The *AtMSH5* gene-specific primers were F1: 5′- GCA CTT GAC TGA GCT ACT TAA CGA GA-3′ and R1: 5′-TGA AAG AAG GCA TGG ATG TCA C-3′. The RT-PCR products were recovered and sequenced to confirm their authenticity and to exclude the possibility of RT-PCR template contamination by genomic DNA.

Characterization of mutant phenotypes

Plants were photographed with a Sony digital camera, DSC-W50 (Sony Corp., Tokyo, Japan). Pictures of the flower were taken using a Nikon SMZ1000 dissecting microscope (Nikon Corp., Tokyo, Japan). To determine pollen viability, mature anthers were stained with Alexander's staining solution [38] and photographed under an Olympus BX-51 microscope (Olympus, Tokyo, Japan). The confocal observation of ovules was performed according to the method described by Christensen *et al*. [39]. Chromosome spreading and DAPI staining were performed as described previously [40]. The number of chiasmata and the number of bivalents/univalents were counted according to the method described by Sanchez-Moran *et al*. [19].

Acknowledgments

This work was supported by the National Natural Science Foundation of China (grant number 30470173). The plant expression vector was kindly provided by Flanders Interuniversity Institute for Biotechnology (VIB), Belgium.

References

1 Kolodner R. Biochemistry and genetics of eukaryotic mismatch repair. *Genes Dev* 1996; **10**:1433-1442.

2 Modrich P. Mechanisms and biological effects of mismatch repair. *Annu Rev Genet* 1991; **25**:229-253.
3 Chi NW, Kolodner RD. Purification and characterization of MSH1, a yeast mitochondrial protein that binds to DNA mismatches. *J Biol Chem* 1994; **269**:29984-29992.
4 Reenan R, Kolodner RD. Characterization of insertion mutations in the *Saccharomyces cerevisiae* MSH1 and MSH2 genes: evidence for separate mitochondrial and nuclear functions. *Genetics* 1992; **132**:975-985.
5 Hollingsworth NM, Ponte L, Halsey C. MSH5, a novel MutS homolog, facilitates meiotic reciprocal recombination between homologs in *Saccharomyces cerevisiae* but not mismatch repair. *Genes Dev* 1995; **9**:1728-1739.
6 Ross-Macdonald P, Roeder GS. Mutation of a meiosis-specific MutS homolog decreases crossing over but not mismatch correction. *Cell* 1994; **79**:1069-1080.
7 Kelly KO, Dernburg AF, Stanfield GM, Villeneuve AM. *Caenorhabditis elegans msh-5* is required for both normal and radiation-induced meiotic crossing over but not for completion of meiosis. *Genetics* 2000; **156**:617-630.
8 de Vries SS, Baart EB, Dekker M, *et al*. Mouse MutS-like protein Msh5 is required for proper chromosome synapsis in male and female meiosis. *Genes Dev* 1999; **13**:523-531.
9 Edelmann W, Cohen PE, Kneitz B, *et al*. Mammalian MutS homologue 5 is required for chromosome pairing in meiosis. *Nat Genet* 1999; **21**:123-127.
10 Bocker T, Barusevicius A, Snowden T, *et al*. hMSH5: A human MutS homologue that forms a novel heterodimer with hMSH4 and is expressed during spermatogenesis. *Cancer Res* 1999; **59**:816-822.
11 Snowden T, Acharya S, Butz C, Berardini M, Fishel R. hMSH4-hMSH5 recognizes Holliday junctions and forms a meiosis-specific sliding clamp that embraces homologous chromosomes. *Mol Cell* 2004; **15**:437-451.
12 Higgins JD, Armstrong SJ, Franklin FC, Jones GH. The *Arabidopsis* MutS homolog AtMSH4 functions at an early step in recombination: evidence for two classes of recombination in *Arabidopsis*. *Genes Dev* 2004; **18**:2557-2570.
13 Her C, Wu XL, Bailey SM, Doggett NA. Mouse MutS homolog 4 is predominantly expressed in testis and interacts with MutS homolog 5. *Mammalian Genome* 2001; **12**:73-76.
14 Sekine H, Ferreira RC, Pan-Hammarström Q, *et al*. Role for Msh5 in the regulation of Ig class switch recombination. *PNAS* 2007; **104**:7193-7198.
15 Sakamoto W, Kondo H, Murata M, Motoyoshi F. Altered mitochondrial gene expression in a maternal distorted leaf mutant of *Arabidopsis* lnduced by *chloroplast mutator*. *Plant Cell* 1996; **8**:1377-1390.
16 Emmanuel E, Yehuda E, Melamed-Bessudo C, Avivi-Ragolsky N, Levy AA. The role of AtMSH2 in homologous recombination in *Arabidopsis thaliana*. *EMBO Rep* 2006; **1**:100-105.
17 Hoffman PD, Leonard JM, Lindberg GE, Bollmann SR, Hays JB. Rapid accumulation of mutations during seed-to-seed propagation of mismatch-repair-defective *Arabidopsis*. *Genes Dev* 2004; **18**:2676-2685.
18 Culligan KM, Hays JB. *Arabidopsis* MutS homologs—AtMSH2, AtMSH3, AtMSH6, and a Novel AtMSH7—form three distinct protein heterodimers with different specificities for mismatched DNA. *Plant Cell* 2000; **12**:991-1002.
19 Sanchez Moran E, Armstrong SJ, Santos JL, Franklin FCH, Jones GH. Chiasma formation in *Arabidopsis thaliana* accession *Wassileskija* and in two meiotic mutants. *Chromosome Res* 2001; **9**:121-128.
20 Biswas I, Hsieh P. Interaction of MutS protein with the major and minor grooves of a heteroduplex DNA. *J Biol Chem* 1997; **272**:13355-13364.
21 Lamers MH, Perrakis A, Enzlin JH, Winterwerp HK, Wind Nd, Sixma TK. The crystal structure of DNA mismatch repair protein MutS binding to a G x T mismatch. *Nature* 2000; **407**:711-717.
22 Obmolova G, Ban C, Hsieh P, Yang W. Crystal structures of mismatch repair protein MutS and its complex with a substrate DNA. *Nature* 2000; **407**:703-710.
23 Hsieh P. Molecular mechanisms of DNA mismatch repair. *Mutat Res* 2001; **4862**:71-87.
24 Yang W, Steitz TA. The recently reported crystal structures of two recombination enzymes, the catalytic domain of HIV integrase and *Escherichia coli* RuvC, an endonuclease, are surprisingly similar to that of ribonuclease H suggesting the possibility that they have a common enzymatic mechanism. *Structure* 1995; **3**:131-134.
25 Timsit Y. Convergent evolution of MutS and topoisomerase II for clamping DNA crossovers and stacked Holliday junctions. *J Biomol Struct Dynamics* 2001; **2**:215-218.
26 Alani E, Sokolsky T, Studamire B, Miret JJ, Lahue RS. Genetic and biochemical analysis of Msh2p-Msh6p: role of ATP hydrolysis and Msh2p-Msh6p subunit interactions in mismatch base pair recognition. *Mol Cell Biol* 1997; **17**:2436-2447.
27 Novak JE, Ross-Macdonald PB, Shirleen Roeder G. The budding yeast Msh4 protein functions in chromosome synapsis and the regulation of crossover distribution. *Genetics* 2001; **158**:1013-1025.
28 Ross-Macdonald P, Shirleen Roeder G. Mutation of a meiosis-specific MutS homolog decreases crossing over but not mismatch correction. *Cell* 1994; **79**:1069-1080.
29 Pochart P, Woltering D, Hollingsworth NM. Conserved properties between functionally distinct MutS homologs in yeast. *J Biol Chem* 1997; **272**:30345-30349.
30 Jackson N, Sanchez-Moran E, Buckling E, Armstrong SJ, Jones GH, Franklin FCH. Reduced meiotic crossovers and delayed prophase I progression in AtMLH3-deficient *Arabidopsis*. *EMBO J* 2006; **25**:1315-1323.
31 Zalevsky J, MacQueen AJ, Duffy JB, Kemphues KJ, Villeneuve AM. Crossing over during *Caenorhabditis elegans* meiosis requires a conserved MutS-based pathway that is partially dispensable in budding yeast. *Genetics* 1999; **153**:1271-1283.
32 Santos Tdl, Hunter N, Lee C, Larkin B, Loidl J, Hollingsworth NM. The Mus81/Mms81 endonuclease acts independently of double Holliday junction resolution to promote a distinct subset of crossovers during meiosis in budding yeast. *Genetics* 2003; **164**:81-94.
33 Copenhaver GP, Housworth EA, Stahl FW. Crossover interference in Arabidopsis. *Genetics* 2002; **160**:1631-1639.
34 Mercier R, Jolivet S, Vezon D, *et al*. Two meiotic crossover classes cohabit in *Arabidopsis*: one is dependent on *MER3*, whereas the other one is not. *Current Biology* 2005; **15**:692-701.
35 Chen Cb, Zhang W, Timofejeva L, Gerardin Yand, Ma H. The

Arabidopsis ROCK-N-ROLLERS gene encodes a homolog of the yeast ATP-dependent DNA helicase MER3 and is required for normal meiotic crossover formation. *Plant J* 2005; **43**:321-334.

36 Berchowitz LE, Francis KE, Bey AL, Copenhaver GP. The role of AtMUS81 in interference-insensitive crossovers in *A. thaliana*. *PLoS Genet* 2007; **3**: e132.

37 Cottage A, Yang A, Maunders H, de Lacy RC, Ramsay NA. Identification of DNA sequences flanking T-DNA insertions by PCR-walking. *Plant Mol Biol Rep* 2001; **19**:321-327.

38 Alexander MP. Differential staining of aborted and nonaborted pollen. *Stain Technol* 1969; **44**:117-122.

39 Christensen CA, King EJ, Jordan JR, Drews GN. Megagametogenesis in Arabidopsis wild type and the Gf mutant. *Sex Plant Reprod* 1997; **10**:49-64.

40 Ross KJ, Fransz P, Jones GH. A light microscopic atlas of meiosis in *Arabidopsis thaliana*. *Chromosome Res* 1996; **4**:507-516.